

Jordan Journal of Physics

ARTICLE

Influence of Current Density on Morphology of Electrochemically Formed Porous Silicon

Ammar M. Al-Husseini

Department of Physics, The University of Jordan, Amman 11942, Jordan.

Received on: 14/1/2016; Accepted on: 6/4/2016

Abstract: Porous silicon samples were prepared by electrochemical anodic etching of p-type silicon wafer in hydrofluoric (HF) acid-based solution. The electrochemical process allowed precise control of porous silicon properties, such as average pore diameter, average pore depth and porosity. The effect of current density on physical properties of porous silicon was investigated by Scanning Electron Microscopy (SEM), I-V characteristics and Fourier Transform Infrared (FTIR) spectroscopy. The average pore diameter and average pore depth were found to increase with the increase in current density. The average pore diameter varied from (10 to 28) nm and the average pore depth varied from (470 to 2200) nm, when the current density was changed from (5 to 36) mA/cm² for 10 minutes. In addition, Al/porous/crystalline silicon sandwich showed a good rectification device.

Keywords: Porous silicon, Electrochemical etching, Current density, SEM, FTIR, I-V characteristics.

Introduction

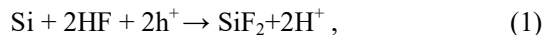
Porous silicon is an important material for applications in microelectronics. Since Uhler and Tumer [1, 2] first reported in the late 1950s that silicon surface can be covered with a brown film during anodization in HF solutions [3], porous silicon was found to form by electrochemical etching of p or n doped mono-crystalline silicon in hydrofluoric acid (HF) [4]. The microstructural and physical characteristics of porous silicon, such as thickness, pore diameter, pore distribution and specific surface area are critically dependent on various processing conditions, etching solution composition, current density, etching time, illumination and properties of the silicon substrate, such as doping level and crystal orientation [4-8]. In general, porous silicon (PS) obtained by anodization of a silicon wafer is a versatile material which can display different morphologies by varying the doping density of the wafer as well as the formation parameters. Nanoporous silicon (2–4 nm) can be generally achieved by using p-type as well as

n-type silicon of low and moderate doping density. Mesoporous silicon with pore diameters from 5 to 50 nm is generally formed utilizing highly doped silicon as substrate, and for macropore (>50 nm up to a few μm) formation moderately doped silicon is usually employed [9]. All these different types of porous silicon are used in basic research studies, but are also appropriate for potential applications.

Porous silicon; a versatile material with various morphological natures, is compatible to today's microtechnology and is of interest for a great variety of applications. The high surface area of this material (nanoporous silicon $\sim 1,000 \text{ m}^2/\text{cm}^3$, mesoporous silicon $\sim 100 \text{ m}^2/\text{cm}^3$ and macroporous silicon $\sim 1 \text{ m}^2/\text{cm}^3$) makes it suitable to fill the pores with one or more guest materials, which results in a drastic change of the physical properties [10].

In order to form porous silicon, the current at the silicon side of the silicon/electrolyte interface must be carried by holes, injected from the bulk

towards the interface. Several different mechanisms regarding the solution chemistry of silicon have been proposed, but it is generally accepted that holes are required for pore formation [11]. The global anodic semi-reaction can be written during pore formation as:



The etching rate is determined by holes (h^+) accumulating in the adjacent regions of the HF electrolyte and Si atoms [3, 6, 7 and 12]. Porous silicon is a promising material due to excellent optical, mechanical and thermal properties, compatibility with silicon-based microelectronics [13] and low cost [14]. All these features have led to many applications of porous silicon, such as solar cells, gas sensors, pressure sensors, bio-sensors, photovoltaic devices, ...etc. [15-19]. The interest in porous silicon has increased greatly over the past decades, mainly due to its photoluminescence properties and the potential applications arising from these [20]. Technological application of porous silicon (PS) as a light

emitter would have a significant impact on numerous technologies, such as light emitting devices [21], micro-cavities[22], wave guides and solar cells[23,24]. Porous silicon (PS) is an interesting material for gas sensing applications [25, 26].

In this paper, scanning electron microscopy (SEM) is used to study the influence of etching current density on pore diameter and pore depth for mesoporous silicon.

Experimental Details

The experiment setup of electrochemical etching is illustrated in Fig. 1. A constant current is supplied between two electrodes immersed in Teflon cell (highly acid-resistant material) containing an aqueous solution of hydrofluoric acid HF (49%), ethanol $\text{C}_2\text{H}_5\text{OH}$ (99%) and deionized water H_2O . Adding ethanol to the electrolyte produces more homogenous structures. Ethanol removes hydrogen bubbles induced during the electrochemical reaction, making the porous structures more uniform [6].

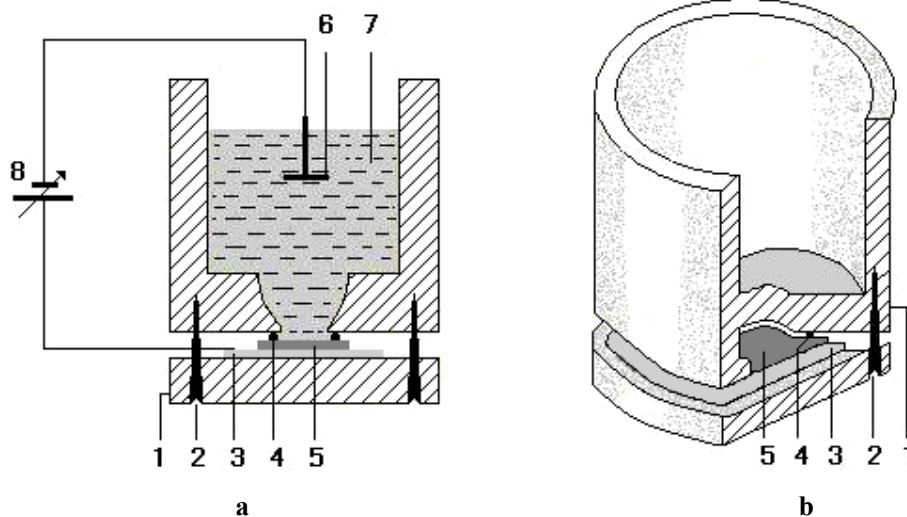


FIG. 1. Electrochemical etching experimental setup: (a) schematic view, (b) cross-section of the electrochemical etching tank. 1- Teflon container, 2- screw, 3- aluminum anode, 4- O-ring, 5- silicon wafer, 6- platinum cathode, 7- electrolyte, 8- variable power supply.

The substrate used was mono-crystalline p-type silicon (100) oriented, with 3-30 Ωcm resistivity and a thickness of $675 \pm 25 \mu\text{m}$. The silicon wafers were cleaved into 4cm squares (few mm larger than the O-ring used in the etching container) to ensure a leak-free seal. The silicon samples were placed at the bottom of the cylindrical Teflon container and fixed by an aluminum plate as backing material, so that the

current required for the etching process could pass from the bottom surface to the top of the polished surface via the electrolyte. Platinum plate represents the cathode which was placed perpendicular to the silicon surface at a distance of 2cm. The porous layers on the surface of these samples were prepared at current densities of 5, 10, 20 and 36 mA/cm^2 for 10 min etching time. After etching, the samples were thoroughly

rinsed with ethanol (twice or more) to remove any HF trace. Finally, the samples were examined using FIE Scanning Electron Microscope (SEM), Keithly electrometer I-V characteristics and Thermo Nicolet Fourier Transform Infra-Red (FTIR) spectroscopy in order to verify precisely pore formations on the silicon membrane.

Results and Discussion

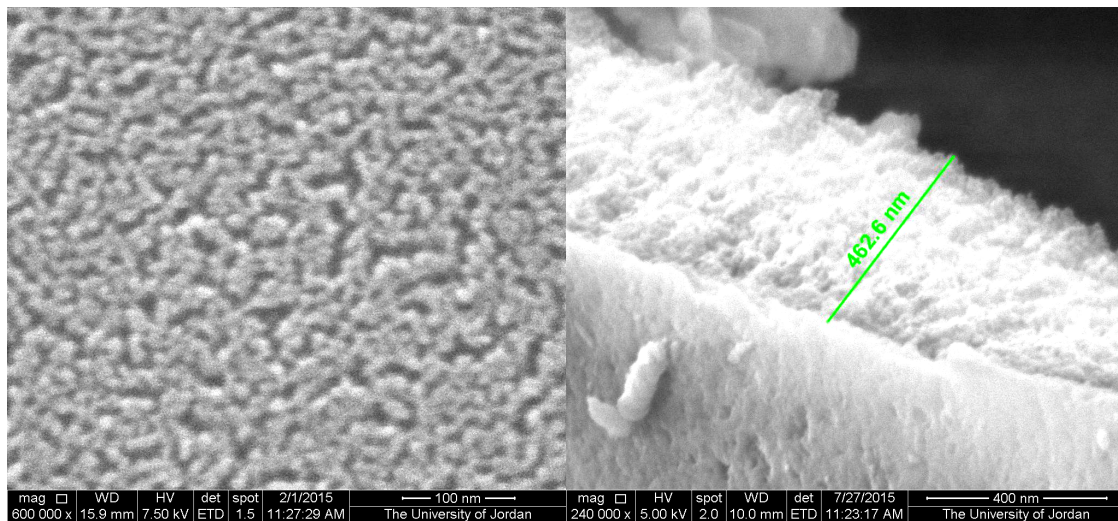
Fig. 2 shows the top view and cross-section SEM images of the porous silicon, prepared by electrochemical etching of p-type silicon wafers for 10 minutes. The electrolyte consists of 1(49%) HF: 2(99%) C₂H₅OH:2 H₂O, using different current densities of 5, 10, 20 and 36 mA/cm². With the help of the surface images of the samples, the dark spots on the images are attributed to the pores formed, whereas the white area corresponds to the remaining silicon. The pores are spherical and irregular in shape and are randomly distributed on the porous silicon surface. Porous silicon formed at different current densities has different pore sizes. At a current density of 5 mA/cm², pores were 9-11 nm in diameter and 420-500 nm in depth (Fig. 2 a). For current density of 10 mA/cm², the pore diameter was 15-17 nm, while pores were 630-710 nm in depth (Fig.2 b). The use of 20 mA/cm² current density resulted in pore diameter of 18.4 -20.0 nm and pore depth of 1260-1400 nm (Fig. 2c). Finally, at a current density of 36 mA/cm², the pore diameter became 27-29 nm and the pore depth was 2130-2300 nm (Fig. 2d).

Fig. 3 shows the distribution of pore sizes for a sample prepared using a current density of 10 mA/cm², for which the average pore diameter was 16 nm with a standard deviation of 0.6 nm.

The variation in the average pore diameter of porous silicon with etching current density is illustrated in Fig. 4. As can be seen, the pore diameter increases exponentially with current density [27]. The current density was changed from 5 mA/cm² to 36 mA/cm² and the average pore diameter increased from 10 nm to 28 nm. The average pore diameters were determined via manual measurement of at least twenty pores randomly selected from two different SEM images. The average pore diameters appear to be in good agreement with what is expected for meso-pore layer [9,10]. The variation in the average pore depth of porous silicon with etching current density is illustrated in Fig. 5. The average pore depths were determined via manual measurement of at least ten pores randomly selected from two different SEM images. When the current density was changed from 5 mA/cm² to 36 mA/cm², the average pore depth increased from 470 nm to 2200 nm. Pore depth generally increases with increasing current density, because increasing current density produces excess electron-hole pairs and subsequently enhances the porous silicon thickness layer [11, 28]. In fact, the relation between pore depth and current density has been predicted to be of the form:

$$d_{\text{pore}} = (1.2)(J)^{0.8}, \quad (3)$$

where d_{pore} is the pore depth and J is the current density.



(a)

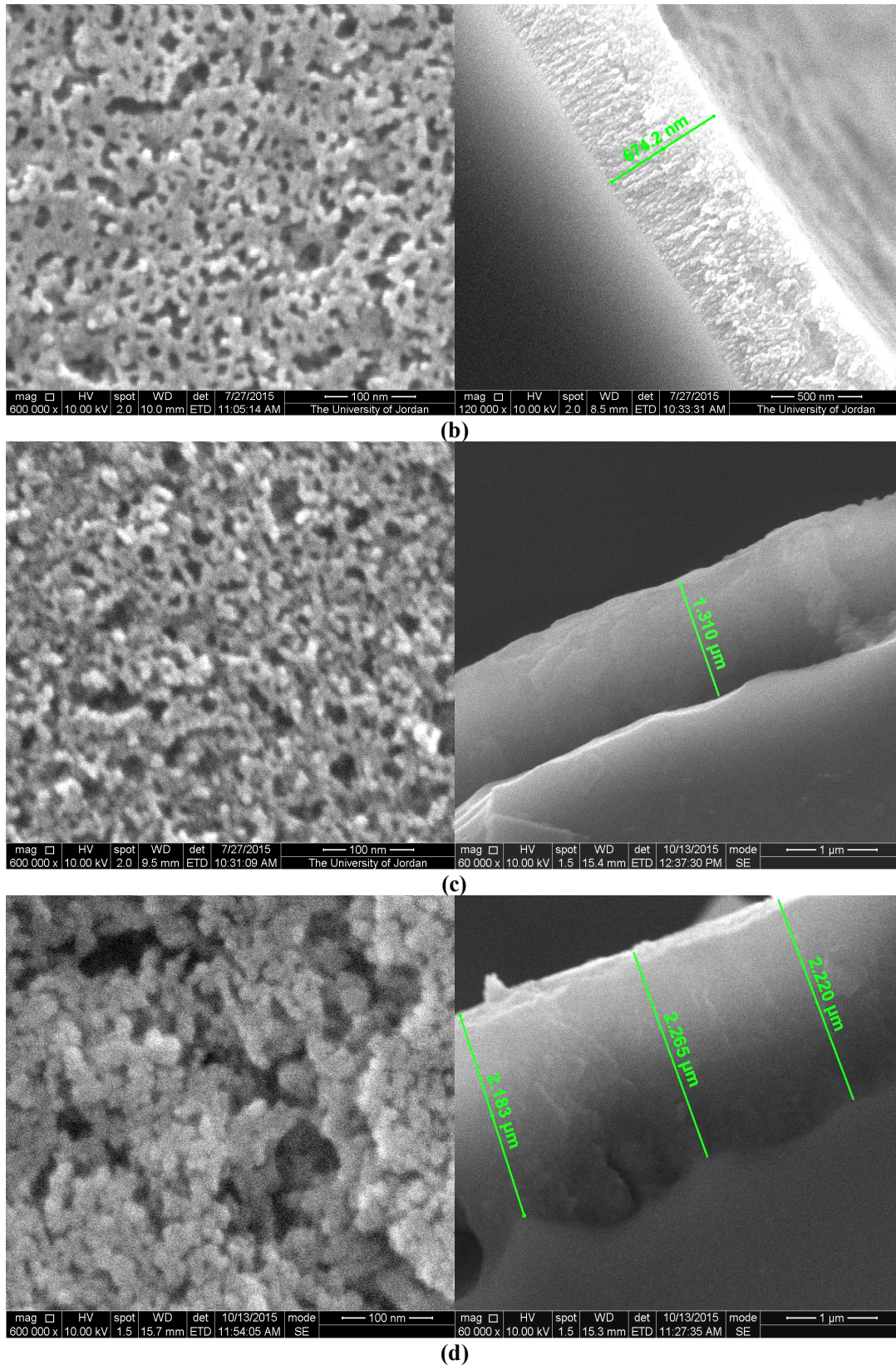


FIG. 2. Top view and cross-section SEM images of the porous silicon samples. The samples were prepared by p-type (100) orientation in electrolyte consisting of HF:C₂H₅OH:H₂O in the ratio of (1:2:2) by volume with an etching time of 10 minutes, (a) current density = 5 mA/cm², (b) current density = 10 mA/cm², (c) current density = 20 mA/cm², (d) current density = 36 mA/cm².

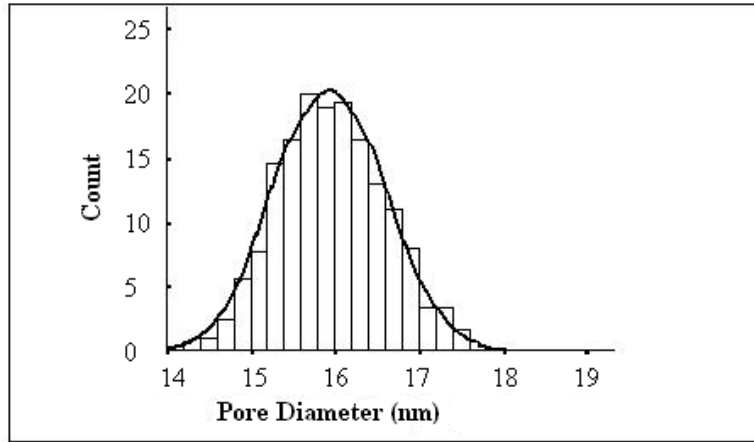


FIG. 3. Pore size distribution for a porous silicon sample formed at a current density of 10 mA/cm². Data from two different SEM images was used.

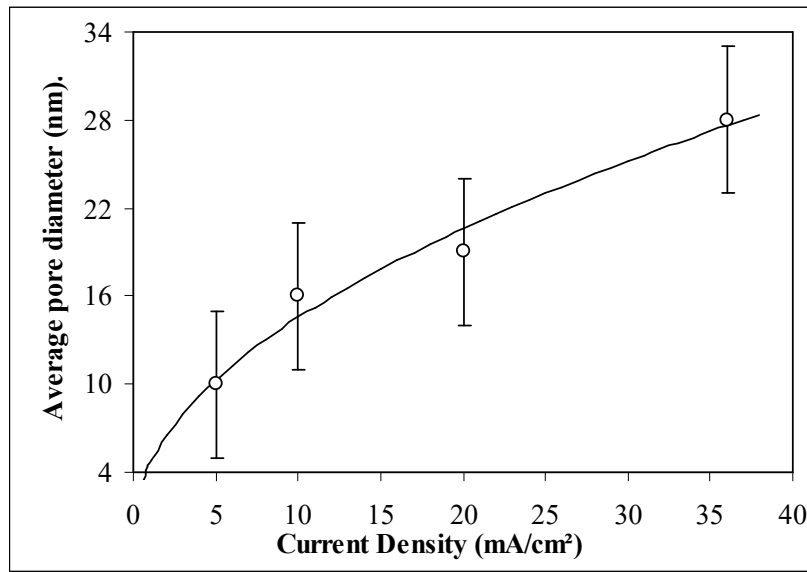


FIG. 4. Average pore diameter as a function of current density.

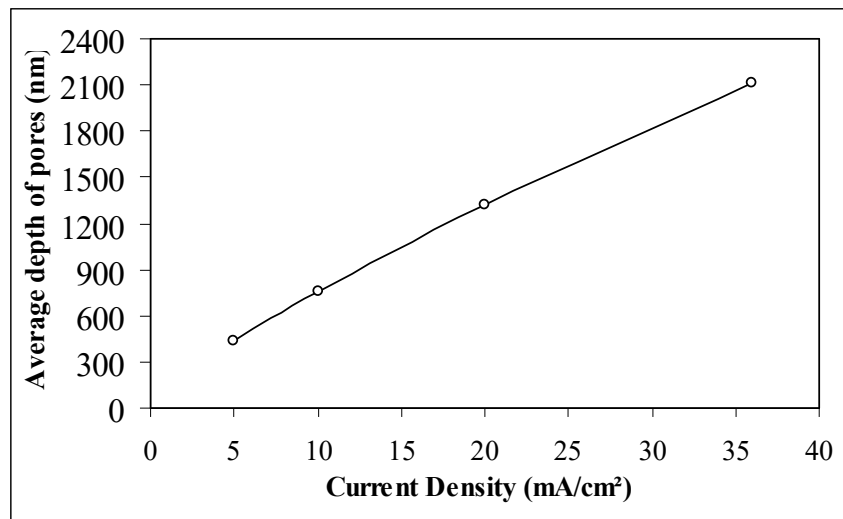


FIG. 5: Average depth of pores as a function of current density.

I-V Characteristics

Fig. 6 shows current-voltage (I-V) characteristics for Al/porous silicon/crystalline/Al sandwich structure device. These were measured under illumination conditions as a function of different etching current densities (5mA/cm^2 and 20mA/cm^2) and 10 minutes etching time. Keithly electrometer (model 6517A) was used to measure the current-voltage (I-V) characteristics. The (I-V) curves were obtained by applying a varying bias voltage (from -5V to $+5\text{V}$). The variation in forward bias characterization is controlled by porous silicon layer resistance. This result explains the reduction of flow current in forward bias with

increasing the etching current density [29]. The pore diameter increases as etching current density increases and hence the resistance of porous silicon layer becomes too high. This will reduce the forward current density. When the pore diameter increases, the pore wall which acts as a carriers' trap will increase to form a high resistive region which decreases the current passing through the porous silicon layer. Also, increasing the etching current density from 5mA/cm^2 to 20mA/cm^2 will lead to increase the thicknesses of the porous silicon layer. Increasing the thickness of the porous silicon layer will lead to increase its resistivity due to reduced mobility in it [30-33].

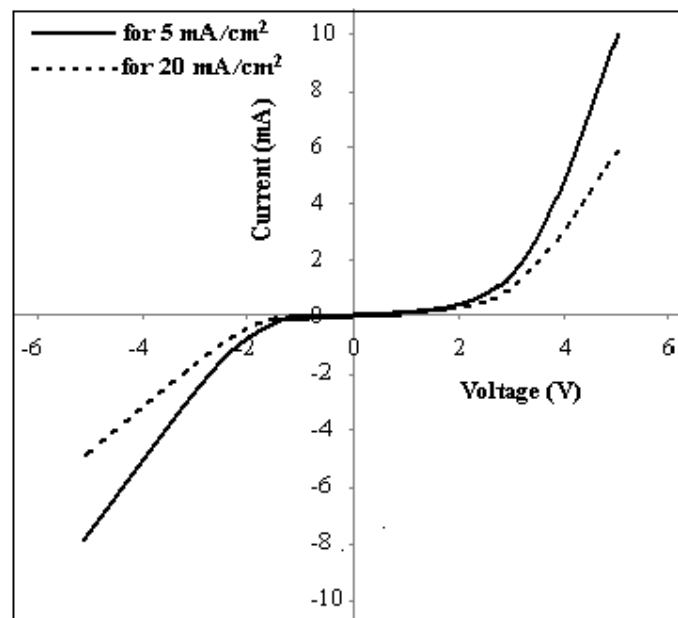


FIG. 6. I-V characteristics of Al/porous silicon/crystalline silicon/Al sandwich structure device.

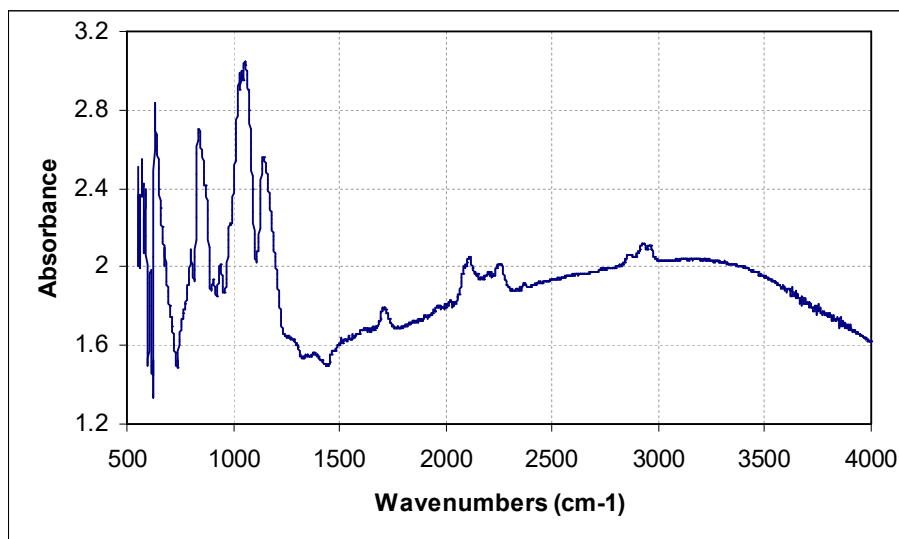
Fourier Transform Infra-Red (FTIR) Study

Fourier Transform Infrared (FTIR) spectroscopy has been widely used as a tool for characterization of chemical bonding, especially extensively in porous silicon. Thermo Nicolet 670 FT-IR spectroscopy was utilized in this study to characterize the active vibrational bonds in the porous silicon sample. The system covers the range ($500\text{-}4000\text{ cm}^{-1}$) at room temperature. When infrared radiation interacts with the sample, the chemical bonds will stretch, contract and bend. As a result, the bonds will tend to absorb the infrared radiation at different wavelengths.

Fig. 7 shows the FTIR absorbance spectrum of porous silicon at a current density of 10mA/cm^2 and an etching time of 10 minutes. The peaks are: 624.94 cm^{-1} Si-Si bonds vibration, 837.62 cm^{-1} Si-H₂ wagging mode and 940.21 cm^{-1} Si-H₂ scissor mode. The peaks around 1051.22 cm^{-1} and 1144.45 cm^{-1} are related to Si-O-Si stretching modes. The peaks at 2120.74 cm^{-1} and 2903.27 cm^{-1} are, respectively, related to Si-H stretch and C-H stretch. Chemical bonds and their IR resonance positions detected in porous silicon are shown in Table (1). The FTIR peaks are in good agreement with other reported results [34, 35].

TABLE 1. Bonds in porous silicon spectrum at a current density of 10 mA/cm² and an etching time of 10 min.

Wave number (cm ⁻¹)	Bonds	Vibration modes
634.50	Si-Si	Stretching
837.62	Si-H ₂	Wagging
940.21	Si-H ₂	Scissor
1051.22	Si-O-Si	Stretching
1144.45	Si-O-Si	Stretching
2120.74	Si-H	Stretching
2903.27	C-H	Stretching

FIG. 7. FTIR spectrum of porous silicon at a current density of 10 mA/cm² and an etching time of 10 min.

Conclusions

Porous silicon samples were prepared by electrochemical etching method at various current densities. The results show that the diameter and depth of the pores were substantially affected by the etching current density. The Scanning Electron Microscopy (SEM) investigation shows that the average pore diameter and depth are increasing with the increase of etching current density. I-V characteristics of Al/porous silicon/crystalline silicon/Al sandwich structure device showed

good rectification characteristics. Finally, Fourier Transform Infrared (FTIR) spectroscopy studies revealed vibration, symmetrical stretching, wagging and stretch/bend bonds. These results indicate that the porous silicon is a good candidate for photonic devices.

Acknowledgment

The author would like to thank both Dr. Walid Hamoudi and Dr. Bashar Lahlouh for their helpful discussion.

References

- [1] Uhlir, A., *The Bell Syst. Tech. J.*, 35 (1956) 333.
- [2] Turner, D.R., *J. Electrochem. Soc.*, 105 (1958) 402.
- [3] Zhang, G.X., "Modern Aspects of Electrochemistry", Number 39, edited by C. Vayenas et al., Springer, (New York, 2005) 65-69,155.
- [4] Smith, R.L. and Collins, S.D., *J. Appl. Phys.*, 71 (1992) R1.
- [5] Zangoie, S., Jansson, R. and Arwin, H., *Applied Surface Science*, 136(1-2) (1998) 123.
- [6] Sailor, M.J., Wiley-VCH Verlag and Co. KGaA, Boschstr. 12, 69469, (Weinheim, Germany, 2012) 5-12.

- [7] Kumar, P. and Huber, P., *Journal of Nanomaterials*, (2007) 1.
- [8] Peckham, J. and Andrews, G.T., *Semicond. Sci. Technol.*, 28 (2013) 105027.
- [9] Chazalviel, J.-N., Ozanam, F., Gabouze, N., Fellah, S. and Wehrspohn, R.B., *J. Electrochem. Soc.*, 149 (2002) C511.
- [10] Granitzer, P. and Rumpf, K., *Materials*, 3 (2010) 943, doi:10.3390/ma3020943.
- [11] Pérez, E.X., *Design, Fabrication and Characterization of Porous Silicon Multilayer Optical Devices*, ISBN: 978-84-691-0362-3/DL: T.2181, (Universitat Rovira I Virgili, 2007).
- [12] Zhang, X.G., *Journal of the Electrochemical Society*, 151(1) (2004) C69.
- [13] Hirschman, K.D., Tsybeslov, L., Duttaguola, S.P. and Fauchet, P.M., *Nature*, 384 (1996) 338.
- [14] Behzad, K., Yunus, W.M.M., Talib, Z., Zakaria, A. and Bahrami, A., *Int. J. Electrochem. Sci.*, 7 (2012) 8266.
- [15] Dubey, R. and Gautum, D., *Opt. Quant. Electron.*, 41 (2009) 189.
- [16] De Stefano, L., Moretti, L., Lamberti, A., Longo, O., Rocchia, M., Rossi, A.M., Arcari, P. and Rendina, I., *IEEE Transactions on Nanotechnology*, 3(1) (2004).
- [17] Singh, P., Sharma, S.N. and Ravindra, N.M., *JOM*, 62(6) (2010) 15.
- [18] De Stefano, L. et al., *Sensors*, 7 (2007) 214.
- [19] Mathew, F.P. and Alocilja, E.C., *Biosensors Bioelectron.*, 20 (2005) 1656.
- [20] Kawasaki, K.K., *Material Science and Engineering*, 69(70) (2000) 132.
- [21] Adawiya, J.H., *Iraq J. of Appl. Phys.*, 4(1) (2008) 37.
- [22] Pavesi, L., *Rivista Del Nuovo Cimento*, 20 (1997) 1.
- [23] Lin, T.L. Chen, S.C., Kao, Y.C., Wang, K.L. and Iyer, S., *Applied Physics Letters*, 48(26) (1986) 1793.
- [24] Bilyalov, R.R. et al., *Sol. Eng. Mater. Sol. Cells*, 65 (2001) 477.
- [25] Canham, L., "Porous Silicon Application Survey", IEE Inspec., (London, U.K., 1997) 364.
- [26] Alwan, A.M., Haider, A.J. and Jabbar, A.A., *Surface and Coating Technology*, 283 (2015) 22.
- [27] Haldar, S., De, A., Chakraborty, S., Ghosh, S. and Ghanta, U., *Procedia Materials Science*, 5 (2014) 764.
- [28] Foll, H., Carstensen, J. and Frey, S., *Journal of Nanomaterials*, (2006) 10.
- [29] Arce, R.D., Koropecki, R.R., Olmos, G., Gennaro, A.M. and Schmidt, J.A., *Thin Solid Films*, 510 (2006) 169.
- [30] Algun, G. and Arikan, M.C., *Tr. J. of Physics*, 23 (1999) 789.
- [31] Chorin, M.B., Moller, F. and Koch, F., *J. Appl. Phys.*, 77(9) (1995) 4482.
- [32] Algun, G. and Arikan, M.G., *J. Phys.*, 23 (1999) 789.
- [33] Abd, H.R., Al-Douri, Y., Ahmed, N.M. and Hashim, U., *Int. J. Electrochem. Sci.*, 8 (2013) 11461.
- [34] Prokes, S.M. and Glembocki, O.J., *Phys. Today*, 83 (1997).
- [35] Mawhinney, D.B. and Yales, J.T., Jr. *J. Phys. Chem. B*, 101 (1997) 1202.